Article

Rapid Diagnosis of Nitrogen Nutrition Status in Summer Maize over Its Life Cycle by a Multi-Index Synergy Model Using Ground Hyperspectral and UAV Multispectral Sensor Data

Abstract: Global climate change and the spread of COVID-19 have caused widespread concerns about food security. The development of smart agriculture could contribute to food security; moreover, the targeted and accurate management of crop nitrogen is a topic of concern in the field of smart agriculture. Unmanned aerial vehicle (UAV) spectroscopy has demonstrated versatility in the rapid and non-destructive estimation of nitrogen in summer maize. Previous studies focused on the entire growth season or early stages of summer maize; however, systematic studies on the diagnosis of nitrogen that consider the entire life cycle are few. This study aimed to: (1) construct a practical diag-nostic model of the nitrogen life cycle of summer maize based on ground hyperspectral data and UAV multispectral sensor data and (2) evaluate this model and express a change in the trend of nitrogen nutrient status at a spatiotemporal scale. Here, a comprehensive data set consisting of a time series of crop biomass, nitrogen concentration, hyperspectral reflectance, and UAV multispectral reflectance from field experiments conducted during the growing seasons of 2017–2019 with summer maize cultivars grown under five different nitrogen fertilization levels in Beijing, China, were considered. The results demonstrated that the entire life cycle of summer maize was divided into four stages, viz., V6 (mean leaf area index (LAI) = 0.67), V10 (mean LAI = 1.94), V12 (mean LAI = 3.61), and VT-R6 (mean LAI = 3.94), respectively; moreover, the multi-index synergy model demonstrated high accuracy and good stability. The best spectral indexes of these four stages were GBNDVI, TCARI, NRI, and MSAVI2, respectively. The thresholds of the spectral index of nitrogen sufficiency in the V6, V10, V12, VT, R1, R2, and R3–R6 stages were 0.83–0.44, −0.22 to −5.23, 0.42–0.35, 0.69–0.87, 0.60–0.75, 0.49–0.61, and 0.42–0.53, respectively. The simulated nitrogen concentration at the various growth stages of summer maize was consistent with the actual spatial distribution.

Keywords: hyperspectral sensor; UAV multispectral sensor; nitrogen concentration; synergy model; summer maize

1. Introduction

Considering global climate change and the COVID-19 pandemic, crops affected by droughts, floods, pests, diseases, and lack of nutrients such as Nitrogen (N) have garnered more attention [1–4]. Nitrogen is essential for crop growth and development [5]. Using remote sensing technology to estimate nitrogen content, existing relevant studies mainly focus on nodes in a certain growth period, which makes it difficult to support relevant business requirements. Maize is one of the most widely planted crops worldwide, grown in over 170 countries. China is the second largest corn producer globally; moreover, summer corn dominates the Huang-Huai-Hai plain in China. Therefore, the fixed-point production

and management of nitrogen that considers the entire life cycle of summer maize is of greatsignificance. Site-specific crop-production management (SCM) is an information-basedtechnology for agricultural production management [6]. Nitrogen is a vital nutrient forsummer maize production in the North China plain; however, excessive fertilization hasadverse effects on the environment [7–9]. The nitrogen demand of summer maize variesspatially across fields, which could lead to localized differences in plant growth [10,11].Hence,nitrogenmanagementisaprimaryconsiderationinSCM[12,13].Anaccurateandrapid monitoring of the nitrogen concentration in crops during the plant life cycle is key toassessing crop nitrogen nutrition and for the SCM of nitrogen fertilizer [14]. It is also a keymethodforreducingtheriskofenvironmentalpollutioncausedbyimproperfertilization management[15,16].

Field variability can be evidenced by maps describing crop status.Maps could beobtained as outputs of proximal (unmanned aerial vehicle (UAV)-mounted) and remotesensing techniques using optical sensors [17], which could then be used to interpret thedynamics of plant nitrogen demand during the crop's life cycle [18]. Maps help to undertakethis rapidly and accurately, instead of using destructive and time-consuming ground-plantsamplingandanalyticalmeasurements[19–21].

Varioussatellite-mountedsensorsaresuitableformonitoringacrop'snitrogennutrientstatus, providing information at different levels of spatial (pixels from 300 to 0.3 m) andtemporal (every 1–44 days) resolution [22]. Numerous studies have shown that nitrogen-sensitive bands are concentrated in the visible and near-infrared regions [18]. Furthermore,spectral indices are mainly calculated from the reflectance of visible and near-infrared bandsaccording to ratios, normalization, or certain formulas [23–26]. However, satellite remotesensing data are greatly affected by weather—it is rainy and cloudy during the growingperiodofsummermaize.Itischallengingtoobtainremotesensingdataintimeundercloudy conditions [18,27–30].Furthermore, some authors stress that this technique haslimited operational flexibility for real-time field monitoring or management due to the lowspatialresolutionoftheimagesacquiredandthelongintervalsbetweensatelliterevisits.

Inrecentyears,thelimitationsofremotesensingsatelliteshaveopenedupnewopportunities for the innovative use of unmanned aerial vehicles (UAVs) in crop monitoring.Equipped with multispectral digital cameras, these devices can be used to periodically flyover a field to obtain spectral information on crops in the visible and near-infrared regionsandcalculatethevegetationindexwithveryhighspatialresolution(usually<20mm).

UAVsareeasytocarryandoperateandcanhelprealizethereal-timemonitoringof nutrients and water management [31], weed control, disease, and pest detection andcan give an estimation of the grain yield [22,32] of different crops (such as rice [33,34],wheat [35], maize [36], etc.), thus providing a guarantee for the SCM. With the adventof robust and reliable unmanned aircraft and low-payload spectral scanners [23,37–39],anopportunitynowexistsforusinghigh-resolutionhyperspectralimagingtechniquestopredict the nitrogen nutrition status of summer maize [23–25,28,40]. However, due to thehigh correlation of adjacent bands in a hyperspectral sensor, the redundant informationis relatively increased. In comparison, the number of multispectral sensor bands are lessthan the hyperspectral ones, with 3 to 10 bands (generally divided into the red, green, blue,visible, thermal infrared (two bands), near-infrared, and panchromatic bands), while re-dundant information is relatively reduced [41,42]. Additionally, the hyperspectral imagingtechnology of UAVs requires specific flight conditions and expensive equipment, contribut-ing to high data acquisition costs and limited promotion and application of low-altitudeaccurate observations [37].The UAV multispectral technology has garnered considerableattention due to its flexibility, convenience, and low cost. In particular, in comparison tonear-surface hyperspectral point measurements, it is also attractive with regard to its scalecapabilities for nitrogen management [15,20,38,43].

Numerousscholarshaveproposedmanyspectralindicesforvariousresearchareas,crops, and growth stages [23–26]. Numerous diagnostic studies on the spectral nitrogennutritionstatusofsummermaizewerealsoundertaken;however,theyprimarilyfocused

on one or several key growth stages [44]. Studies that consider the nitrogen nutrition statusduring the entire life cycle of summer maize are lacking. Most of them consider multiplelinear support vector machines, machine learning language, and other methods to studyandanalyzecropnitrogenspectraldiagnosticmodels. Researchonasimpleandpracticaluniversalmodelislacking.

So far, the application of spectral technology in diagnosing summer maize nitrogenhas primarily focused on single spectral technology, such as by only considering groundhyperspectral research, UAV research, or remote sensing research.Some researchershave combined ground hyperspectral technology with satellite remote sensing technology;however, few have combined ground hyperspectral technology with UAV multispectraltechnology.Previousstudieshavenotedthatspectralindicesaredevelopedfortheentiregrowing season of crops; hence, they could overestimate or underestimate plant parametersatspecificgrowthstages.Forprecisionfarming,exponentsbasedongrowthstages couldbe required to prevent the smoothing that could occur when an entire seasonal equation isapplied to a particular stage [45]. Additionally, spectral tests generally occur in cycles of1–2years;moreover,inter-annualchangesalsoneedtobestudiedanddiscussed.

Therefore, ground hyperspectral technology and UAV multispectral technology werecombined here to diagnose the nitrogen nutrition status over the entire life cycle of summermaize. This study aimed to: (i) construct and evaluate a diagnostic model of nitrogen con-sidering the entire life cycle of summer maize using systematic near-surface hyperspectraldata from 2017 to 2019; (ii) optimize the summer maize life cycle nitrogen diagnostic modelusingUAVmultispectraldatafrom2019;and(iii)determinethespectralindexthresholdsofsufficientandinadequateplantnitrogennutritionnutrientlevelsatdifferentstagesofthe summer maize life cycle based on the optimized nitrogen diagnostic model and thecriticalnitrogenconcentrationmodel.

2. MaterialsandMethods

2.1. FieldExperimentsandEnvironmentalConditions

Field experiments were conducted in the China National Research Center of Water-savingIrrigationEngineeringTechnology,DaxingDistrict,Beijing,China(39°39′N,116°15′E,34 m above sea level) in three consecutive growing seasons (2017–2019). Daxing is locatedwithin semiarid-temperate, continental monsoon climate zones. The soil at the experimentalsite was classified as a tidal soil comprising a silty loam in the 0–100 cm soil layer.Theaverage soil bulk density in the 0–60 cm soil layer is 1.42 g cm^{-3}.The average nitratenitrogen content,ammonia nitrogen content,and PH value are 20.44 mg kg^{-1},5.20 mgkg^{-1}, and 8.2, respectively, before the summer maize sowing. The mean annual temperatureis 13.4 °C and the mean annual precipitation is 532 mm. The three experimental seasonswere characterized by varying environmental conditions, with major differences in rainfallandtemperature,especiallyforJuly(beginningofthegrowingperiodinsummer)andSeptember(endofthegrowingperiodinautumn).InFigure1,thecumulativerainfall(mm) and mean temperatures (°C) of the three experimental seasons are presented withvaluesofthelong-termmean(1990–2019).

Arandomblockdesignwiththreereplicationswasused.Theareaofeachplotwas60m^2,withaplantingdensityof55,000plantsperha^{-1}.Thedistributionobtainedwas maintained during the three years,preventing interference of the residual mineralnitrogen. The soil surrounding each plot was insulated to ensure that the fertilizer did notpenetrate the other plots.The field experiment area was surrounded by a 5 m protectedarea. Cultivation and sowing were carried out simultaneously in accordance with the localuniform farming model. The terrain is flat. The soil is uniform in texture and fertility. Themaize plant spacing was 30 cm and the row spacing was 60cm.In all three seasons,awidely grown Chinese summer maize cultivar (Jiyuan 168) was sown on 11 June in 2017,and on 15 June in 2018 and 2019 at five levels of N fertilization (0 (N0), 140 (N1), 209 (N2),279 (N3), and 419 (N4) kgNha^{-1}) with three replications. The N fertilizer was split intotwodosesinaratioof1:3(beforesowingandthetasseling(VT)stageofsummermaize)

and applied on 8 June and 9 August in 2017, on 12 June and 13 August in 2018, and on12 June and 5 August in 2020. Prior to sowing, "keba" compound fertilizer (15% N) wasapplied.In the V12 stage, urea fertilizer (47% N) was applied.Due to a severe watershortage, 60 mm irrigation was undertaken prior to sowing in all three years of the fieldtrials.Weeds,pests,andpathogenswerefrequentlymonitoredandcontrolledasneeded. Thesummermaizewasharvestedon24Septemberin2017–2019.

The "Jiyuan" 168 cultivar was characterized by a short ripening period, lodgingresistance,goodquality,goodresistance,andanoutstandingyield.InChina,thevariet yiswidelygrowninsummermaizeareas.

Field test data are the basis for the model-adjustment verification, and previousstudies have shown that the most effective model-adjustment parameter data are theobservation data under different environments (including climate and field treatment,etc.)[46].Therefore,thenitrogengradientsetinthisstudywasrelativelylarge.

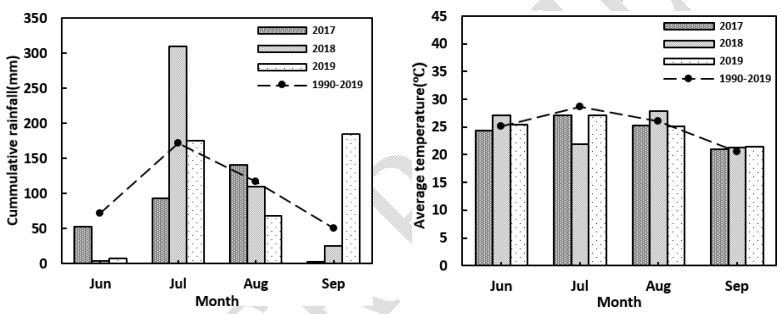

Figure 1. Cumulative rainfall (mm) and mean temperature during the summer maize growingseasons2017–2019inDaxing,Beijing,China.

2.2. PlantSamplingandSpectralMeasurements

Tissue samples were collected to measure the tissue nitrogen concentration in theabove-ground biomass the day after the spectral data were collected.The plants weresampled by cutting the base of the stem just above the soil surface.Additional detailsregarding sample acquisition (i.e., date, stage, sample number, etc.) are listed in supplemen-tary Table S1. Before the annual first test, three representative plants were selected in eachplot and marked as reference plants for each sampling. Three plants were then selected foreach sampling with reference to the plant height, stem diameter, and panicle size of thereference plants. The plant samples were oven-dried at 105 ◦C for 0.5 h and then at 75 ◦Cuntil a constant weight was achieved. Thereafter, the samples were weighed and ground topass through a 1 mm sieve. The nitrogen concentration of the plants was measured usingKjeldahldigestion(TableS2).

Here, spectral reflectance includes hyperspectral reflectance and multispectral re-flectance.Hyperspectralreflectancewasmeasuredfrom2017to2019,usingthepassive,non-imaging spectroradiometer, FieldSpec HandHeld 2 (ASD Inc., Boulder, CO, USA).This device provides hyperspectral data within a wavelength range of 325–1075 nm at asampling interval of 1.5 nm. The spectral sampling dates were synchronized with the plantsampling dates; moreover, the spectral measurements were undertaken on sunny daysaroundmidday(10:00–14:00)Beijingtimeunderclearskyconditions.Thesensorhadafield ofviewof25◦.AfteroptimizationoftheASDinstrument,thereflectanceofthedevicewas set to 100% by measuring the reflectance of a spectral on a reference panel (white referencepanel 25.425.4 cm, calibrated as 99% reflective). The white reference was measuredapproximately every 5–10 min to check the instrument's stability for 100% reflectance.

Thewhitereferencemeasurementswereconductedbybringingthesensorclose(~0.4m)toas pectraltoensurethatthereflectanceofonlythereferencepanelwasmeasured.Three

representative points were selected from each test plot; furthermore, the sensor probe waskept vertically downward during measurement.To ensure that maximum information ontheplantswasobtainedwithinthemeasuredrange,andtominimizetheinfluenceofthesoil background, the sensor was placed ~20 cm away from the plant canopy. The data wereconverted to five multispectral wavebands centered at 475 nm (blue, bandwidth: 20 nm),560nm(green,bandwidth:20nm),668nm(red,bandwidth:10nm),840nm(nearinfrared,bandwidth: 40 nm), and 717 nm (red edge, bandwidth: 10 nm) by calculating the averagereflectanceofthethreereadingsperwaveband.

Multispectral reflectance was measured through a UAV, equipped with a multispectralsensorin2019.TheplatformusedherecomprisedtheJingweim-M600hexrotorUAVsystem controlled by the open-source flight control Pixhawk (DJI, Shenzhen, China).Atpresent,therearemanykindsofmultispectralsensors(suchastheRedEdgesensor,theDJI Phantom 4 Multispectral Camera, the Parrot Sequoia+, the Sentera 6X, etc.). Through aliterature review and a cost-performance analysis [46–48], the Red Edge sensor (Mica Sense,Seattle, WA, USA) was selected. The focal length of the camera was 5.5 mm, with an imageresolution of 1280 960 pixels.The camera was equipped with five spectral channels,with central wavelengths of 475 nm (blue), 560 nm (green)×668 nm (red), 840 nm (nearinfrared), and 717 nm (red edge); it was also equipped with a 30 cm 30 cm gray plate anda light intensity sensor. The light intensity sensor corrected the image of the external lightduringtheshootingprocess.Thegrayplatehadafixedreflectance;moreover,thisplatewas corrected before and after the UAV measurements.The UAV image acquisition wasconductedonsevenoccasionsbetweenJuly2019andSeptember2019andwassynchronized withthetimeofthegrounddataacquisition.TheUAVimageswereacquiredfrom10amto 12 am, while the flight altitude was set to 60 m.The course was fixed during flight(Figures S1 and S2).The overlap between the course and the side was set to 80%, thegroundresolutionwas4.09cm,andtheflightspeedwas3m/s.Atotalof335imageswere collected after the flight and imported into the Pix4Dmapper software for Mosaic.Thereafter,thereflectivityandorthophotoimagesofthestudyareawereobtainedaftergrayplatereflectivitycorrection.

Multispectraldataofthehyperspectralconversionfromthefirsttwoexperiments (2017and2018)wereusedasthetrainingset,whilethosefromthethirdexperiment(2019)and the multispectral data set obtained by a UAV were, respectively, used for validatingthenewparameters("validationdataset").

2.3. DataProcessingandAnalysis

2.3.1. CalculationofSimulatedMultispectralReflectance

Theequationbelowwasusedtoconvertthenear-groundhyperspectralreflectanceinto multispectral reflectance. Thus, a multispectral model to diagnose nitrogen content intheplantcanopywasconstructed:

$$R \quad \sum_{\substack{\lambda=\lambda_{max}\\ \lambda=\lambda_{min}}} = S_\lambda R_\lambda / \sum_{min}^{\lambda=\lambda_{max}\lambda=\lambda} S \qquad (1)$$

where R represents the reflectivity of the wide band of the simulated multispectral; $\lambda_{min}$and λ_{max}represent the starting and ending wavelengths of the UAV sensor, respectively;$S_\lambda$represents the value of the spectral response function of the sensor at the lambdawavelength; and $R_\lambda$represents the hyperspectral reflectance of the summer maize plantcanopyspectrumatthelambdawavelength[49].

2.3.2. MultispectralIndex

This index is a combination of two or more sensitive bands of vegetation;it helpshighlight the vegetation characteristics. Here, over twenty spectral indices that had a goodcorrelation with the nitrogen concentrations of the crops were selected from the publishedliterature for modeling and for verification of the analysis. Table 1 shows the formulas forcalculatingthesemultispectralindices.

Table1. Multispectral reflectance indices used to estimate nitrogen content of crops in this study.

Number	Multispectral Index	Formula	Literature Source
1	GOSAVI	$(1+0.16)(Rnir-Rg)/(Rnir+Rg+0.16)$	[50]
2	MSR1	$[(Rnir/Rr)-1]/[(Rnir/Rr)^{0.5}+1]$	[51]
3	DVI	$Rnir-Rr$	[52]
4	GDVI	$Rnir-Rg$	[53]
5	VARI	$(Rg-Rr)/(Rg+Rr-Rb)$	[54]
6	GRVI	$(Rnir/Rg)-1$	[54]
7	MNLI	$(1.5R^2nir-1.5Rg)/(R^2nir+Rr+0.5)$	[55]
8	OSAVI	$1.16(Rnir-Rr)/(0.16+Rnir+Rr)$	[56]
9	TCARI	$3[(Rnir-Rr)-0.2(Rnir-Rg)(Rnir/Rr)]$	
10	TCARI/OSAVI	TCARI/OSAVI	
11	RDVI	$(Rnir-Rr)/(Rnir+Rr)^{0.5}$	[57]
12	TVI	$0.5[120(Rnir-Rg)-200(Rr-Rg)]$	
13	SAVI	$1.5(Rnir-Rr)/(Rnir+Rr+0.5)$	[58]
14	RVI	$Rnir/Rr$	[59]
15	EVI	$2.5(Rnir-Rr)/(Rnir+6Rr-7.5Rb+1)$	[60]
16	GNDVI	$(Rnir-Rg)/(Rnir+Rg)$	[61]
17	NPCI	$(Rr-Rb)/(Rr+Rb)$	
	[62]18	MSAVI2 $0.5[(2Rnir+1)-[(2Rnir+1)^2-8(Rnir-Rr)]^{0.5}]$	[63]
19	NDVI	$(Rnir-Rr)/(Rnir+Rr)$	[64]
20	NRI	$(Rg-Rr)/(Rg+Rr)$	[65]
21	NLI	$(R^2nir+Rr)/(R^2nir-Rr)$	[66]
22	BNDVI	$(Rnir-Rb)/(Rnir+Rb)$	[67]
23	BRNDVI	$[Rnir-(Rr+Rb)]/[Rnir+(Rg+Rb)]$	
24	GBNDVI	$[Rnir-(Rg+Rb)]/[Rnir+(Rg+Rb)]$	
25	GRNDVI	$[Rnir-(Rg+Rr)]/[Rnir+(Rg+Rr)]$	
26	PNDVI	$[Rnir-(Rg+Rr+Rb)]/[Rnir+(Rg+Rr+Rb)]$	

Note: Rnir, Rr, Rg, and Rb were spectral reflectance of the near-infrared, red, green, and blue wave segments, respectively.

2.3.3. Critical Nitrogen Content Curve

The critical nitrogen content (Nc) was calculated by Equation (2):

$$Nc = aW_{max}^{-b} \quad (2)$$

where a represents the critical nitrogen content of the plants' aboveground unit biomass; b represents the dilution coefficient of the critical nitrogen content; and W_{max} represents the maximum aboveground biomass of the plants (10^3 kg ha^{-1}). The values of a and b were determined based on the field test data.

2.3.4. Leaf Area Index (LAI)

Three summer maize plants which had been tested by hyperspectral measurement in the plots were sampled. The total leaf area was measured using CanoScan LiDE 300. The LAI was calculated using Equation (3):

$$LAI = \frac{total\ leaf\ area\ of\ plant}{the\ plant\ occupies\ land\ area} \quad (3)$$

2.4. ModelEvaluation

Using regression statistics, quantitative monitoring models were established to determineplantnitrogencontentduringvariousgrowthstagesusingamultispectralindex.Thesimulatedvaluesofthequantitativemonitoringmodelwerecalculatedbythedeterminationcoefficient(R^2),therootmeansquareerror(RMSE),andtherelativeerror(RE).Thesensitivitiesofthedifferentspectralvegetationindicesfordetectingchangesinplantnitrogenconcentrationinthegrowthstageswereteste dbyutilizingthenoiseequivalent(NE)method,asreportedbyViñaetal.[68].Themodelingandanalysiswereundertakenin Microsoft Excel 2010. Nitrogen prediction maps from the UAV data were drawn usingENVIandArcGIS.

2.5. DiagnosisFlowofNitrogenNutritionStatus

Thediagnosisflowofthenitrogennutritionstatusinthisstudyisillustratedin Figure 2. First,threeyearsofnear-surfacehyperspectraldataweresimulatedasmulti-spectraldata.

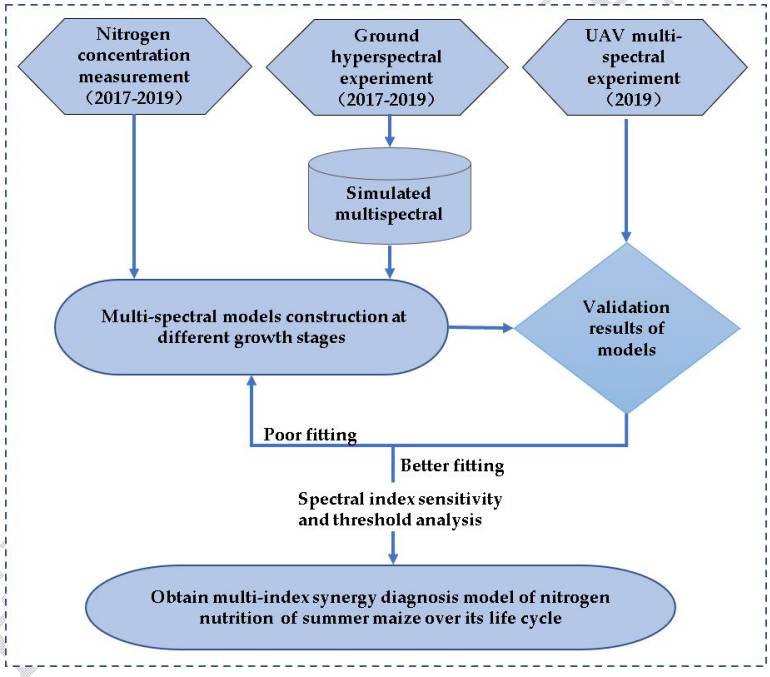

Figure2. Flowchartofdiagnosisofnitrogennutritionstatus.

Furthermore,thewholegrowthstagesofsummermaizeweredividedintodifferentstages, and models were established. The suitable multi-spectral indices for the nitrogennutrition estimation were screened by comparative analysis by using the simulated multi-spectral experiment.In this step, the multi-spectral indices were calculated by usingsimulated spectra, and the relationship between the various multi-spectral indices and thenitrogen nutrition was analyzed to identify the spectral indices that enabled an accurateestimationofthenitrogennutrition.

Finally, the multi-spectral models of nitrogen concentration were validated by theUAVmulti-spectralfieldobservationdata.Itwasconcludedthatthewholegrowthperiodofsummermaizecouldbedividedintoseveralstagesforbetterdiagnosisofthenitrogennutrition.Then,themulti-indexsynergydiagnosismodelofthenitrogennutritionof

summer maize over its life cycle was determined.The sensitivity of these indices toenvironmentalinterferencefactorswasevaluated.Inthisstep,wecalculatedtheLAIandthe criticalnitrogenconcentrationcurveandgavethespectraldiagnostic threshold.

3. Results

3.1. ModelConstructionandOptimization

The ground hyperspectral data measured between 2017 and 2019 were simulated asmultispectral data based on Equation (1). Here, the entire growth period of summer maizewas divided into eight growth stages (V6, V10, V12, VT, R1, R2, R3, and R6); moreover,the relationship between the plant nitrogen concentration and the multispectral index wasestablished using the experimental data for 2017 and 2018. Based on twenty-six commonlyused multispectral indices, the first six spectral indices with good correlation coefficients ineach maize growth period were selected. A model for diagnosing the relationship betweenthe nitrogen concentration and the multispectral indices of the different growth stages wasestablished.Table2showstheresults.

Table 2. Multispectral diagnosis models and evaluation results of the summer maize nitrogenconcentrationatdifferentgrowthstages.

GrowthStage	MultispectralIndex	DiagnosisModel	R^2
V6	GBNDVI	$y=-1.112\ln(x)+2.963$	0.643
	BNDVI	$y=-3.686x+6.488$	0.571
	BRNDVI	$y=-1.194\ln(x)+2.927$	0.536
	PNDVI	$y=-0.560\ln(x)+2.940$	0.472
	NRI	$y=-2.993x+4.297$	0.547
	NDVI	$y=-1.997\ln(x)+3.101$	0.543
V10	TCARI	$y=-0.0998x+2.228$	0.552
	BNDVI	$y=4.8586x-1.6217$	0.448
	TCARI/OSAVI	$y=-0.0874x+2.209$	0.423
	PVI	$y=12.764x+10.388$	0.372
	NPCI	$y=1.725x+2.660$	0.295
	RVI	$y=2.118e^{0.0115x}$	0.274
V12	NRI	$y=-5.833x+4.457$	0.587
	TVI	$y=4.021e^{-0.018x}$	0.395
	DVI	$y=4.029e^{-1.153x}$	0.377
	RDVI	$y=7.343e^{-1.753x}$	0.371
	SAVI	$y=8.028e^{-1.790x}$	0.353
	BNDVI	$y=-6.90\ln(x)+1.545$	0.340
VT	NRI	$y=-2.816x+2.121$	0.424
	OSAVI	$y=-2.525x+3.400$	0.334
	NLI	$y=-1.414x+2.490$	0.331
	RDVI	$y=2.835e^{-1.026x}$	0.323
	SAVI	$y=2.956e^{-1.042x}$	0.315
	MSAVI2	$y=-1.414x+2.489$	0.309

Formatted: Spanish (Mexico)

Table2. *Cont.*

GrowthStage	MultispectralIndex	DiagnosisModel	R^2
R1	DVI	$y=2.983e^{-1.992x}$	0.328
	TVI	$y=2.933e^{-0.031x}$	0.343
	GDVI	$y=3.035e^{-2.170x}$	0.297
	EVI	$y=3.563e^{-1.379x}$	0.235
	MNLI	$y=-1.889x+1.870$	0.229
	RDVI	$y=4.061e^{-1.941x}$	0.227
R2	NDVI	$y=3.544x^{3.731}$	0.376
	MSR1	$y=0.632x^{1.290}$	0.367
	MSR2	$y=0.412x^{1.425}$	0.367
	RVI	$y=0.167x^{1.014}$	0.363
	BRNDVI	$y=3.052x^{1.708}$	0.343
	PVI	$y=586.49e^{16.675x}$	0.279
R3	OSAVI	$y=1.946x^{1.303}$	0.522
	NDVI	$y=1.649x^{1.387}$	0.513
	RVI	$y=0.490\ln(x)+0.153$	0.500
	MSR2	$y=0.815x^{0.605}$	0.498
	MSR1	$y=0.341x+0.380$	0.493
	TCARI/OSAVI	$y=-0.276x+0.934$	0.490
R6	DVI	$y=2.860x^{0.889}$	0.347
	GDVI	$y=3.055x^{0.950}$	0.343
	TVI	$y=0.093x^{0.815}$	0.334
	MNLI	$y=0.690e^{2.654x}$	0.330
	MSAVI2	$y=2.241x^{1.031}$	0.325
	SAVI	$y=2.563x^{1.225}$	0.317

Note:"y%"representedthenitrogenconcentrationofthesummermaizeplant."x"representedmultispectralindices, thesameasbelow.

Table 2 showed that in the different growth stages of summer maize, the multispectralindices were closely related to the nitrogen concentration of the plants; however, they werenotcompletelyconsistent.Thetopsixmultispectralindicesineachstagewereasfollows:in V6:BNDVI, BRNDVI, GBNDVI, PNRI, NRI, and NDVI; in V10:TCARI, TCARI/OSAVI,NPCI, BNDVI, PVI, and RVI; in V12: NRI, BNDVI, TVI, RDVI, DVI, and SAVI; in VT: NRI,OSAVI,NLI,RDVI,SAVI,andMSAVI2;inR1:DVI,GDVI,TVI,MNLI,EVI,andRDVI;inR2: MSR1, RVI, MSR2, NDVI, BRNDVI, and PVI; in R3: OSAVI, NDVI, MSR1, MSR2, RVI,andTCARI/OSAVI;andinR6:GDVI,DVI,MNLI,MSAVI2,TVI,andSAVI.

Thetopsixmultispectralindicesofeachstagewerenonidenticalduetothedifferentenvironments and physiological ecologies of the crops at the different growth stages.Stages V12 and VT were closely related to the multispectral index NRI. Although thecorresponding diagnostic models were linear, the slopes were inconsistent. The slope ofthe~~V~~12stagemodelwas5.833andthatoftheVTs~~ta~~gemodelwas2.816. Thenitrogenconcentration of the plants at the V12 stage varied greatly with the NRI because the nitrogenconcentrationof theseplants wasmore sensitive tochanges inthe NRI.

In the V6, V10, V12, and R3 stages, the determination coefficients of the optimalmultispectral index and plant nitrogen content were mostly above 0.5, while those in the VT,R1,R2,andR6stageswerebasicallybelow0.4.Toimprovetheaccuracyofthemultispectral

Formatted: Spanish (Mexico)
Formatted: Spanish (Mexico)
Formatted: Spanish (Mexico)
Formatted: Spanish (Mexico)
Formatted: Spanish (Mexico)
Formatted: Spanish (Mexico)
Formatted: Spanish (Mexico)
Formatted: Spanish (Mexico)
Formatted: Spanish (Mexico)
Formatted: Spanish (Mexico)

diagnostic model of the nitrogen concentration of summer maize, considering the entiregrowthstageofsummermaize,theLAIchangedgreatlyfromV6toV12(0.34–3.66),whileit changed insignificantly after VT (3.13–4.74). Therefore, stages VT to R6 were combinedintoonestageforremodeling;hence,themodelwasfurtheroptimized(Table3).

Table 3. Multispectral diagnosis models and evaluation results of the summer maize nitrogenconcentrationinthestagesfromVTtoR6.

GrowthStage	MultispectralIndex	Diagnosis	
		Model	R^2
VT-R6	MSAVI2	$y=2.115x^{0.879}$	0.682
	GRNDVI	$y=2.198x^{0.774}$	0.523
	MSR	$y=0.925x^{0.480}$	0.501
	NDVI	$y=2.010x^{1.506}$	0.492
	NRI	y=1.926x+1.092	0.481
	VARI	y=1.190x+1.105	0.452

Aftermodeloptimization,thespectralindexesofthetopsixwereMSAVI2,GRNDVI,MSR, NDVI, NRI, and VARI, respectively. The determination coefficients were all above0.45, and the top one was 0.682.The model determination coefficient was higher than thatoftheindividualmodelsforeachstageofgrowth.Therefore,themultispectraldiagnostic model of plant nitrogen concentration in the whole growth period of summer maize wasdividedintoaneight-stagemodel(V6,V10,V12,VT,R1,R2,R3,andR6)andoptimizedinafour-stagemodel(V6,V10,V12,VT-R6). Theresultsshowedthatthemodelingprecisionwasimprovedbytheoptimizedfour-stagemodel.

3.2. ModelEvaluation

3.2.1. EvaluationofEight-StageModel

This model was evaluated based on the multispectral data converted from the hyper-spectral data and UAV multispectral data of 2019. The accuracy of the top six models inthe different growth stages of summer maize was analyzed using the multispectral dataconverted from the hyperspectral data at eight stages.The equation of the fit betweenthe measured and the predicted values, the determination coefficient R^2, the RMSE, andthe RE is shown in Figure 3.The RMSE of the maize at different growth stages rangedfrom 0.14% to 0.32%, while the RE was <10%; these values indicated that the errors ofthemodelswereinsignificant,whilethestabilityofthesemodelswassuitable. Therefore,themodelfordiagnosingthenitrogenconcentrationofmaizeatdifferentstagescouldbeoptimized by R^2.Generally, a higher $R^2$was selected for the appropriate multispectralindexdiagnosticmodel.

According to Figure 3, the BNDVI spectral index in V6 was prominent in the validationset, with R^2 reaching 0.634. The appropriate spectral index for stage V10 was BNDVI(R^2 = 0.594). NRI (R^2 = 0.573 and 0.342, respectively) was used in both the V12 and the VTstages. TheestimationaccuracyofDVI,GDVI,andTVIintheR1periodwasrelativelyhigh.MSR1, RVI, MSR2, and NDVI could be used during stage R3. The optimal multispectralindex at stage R2 was OSAVI (R^2 = 0.287). MNLI, GDVI, or MSAVI2 could be used as theoptimalmultispectralindexatthematuritystage.

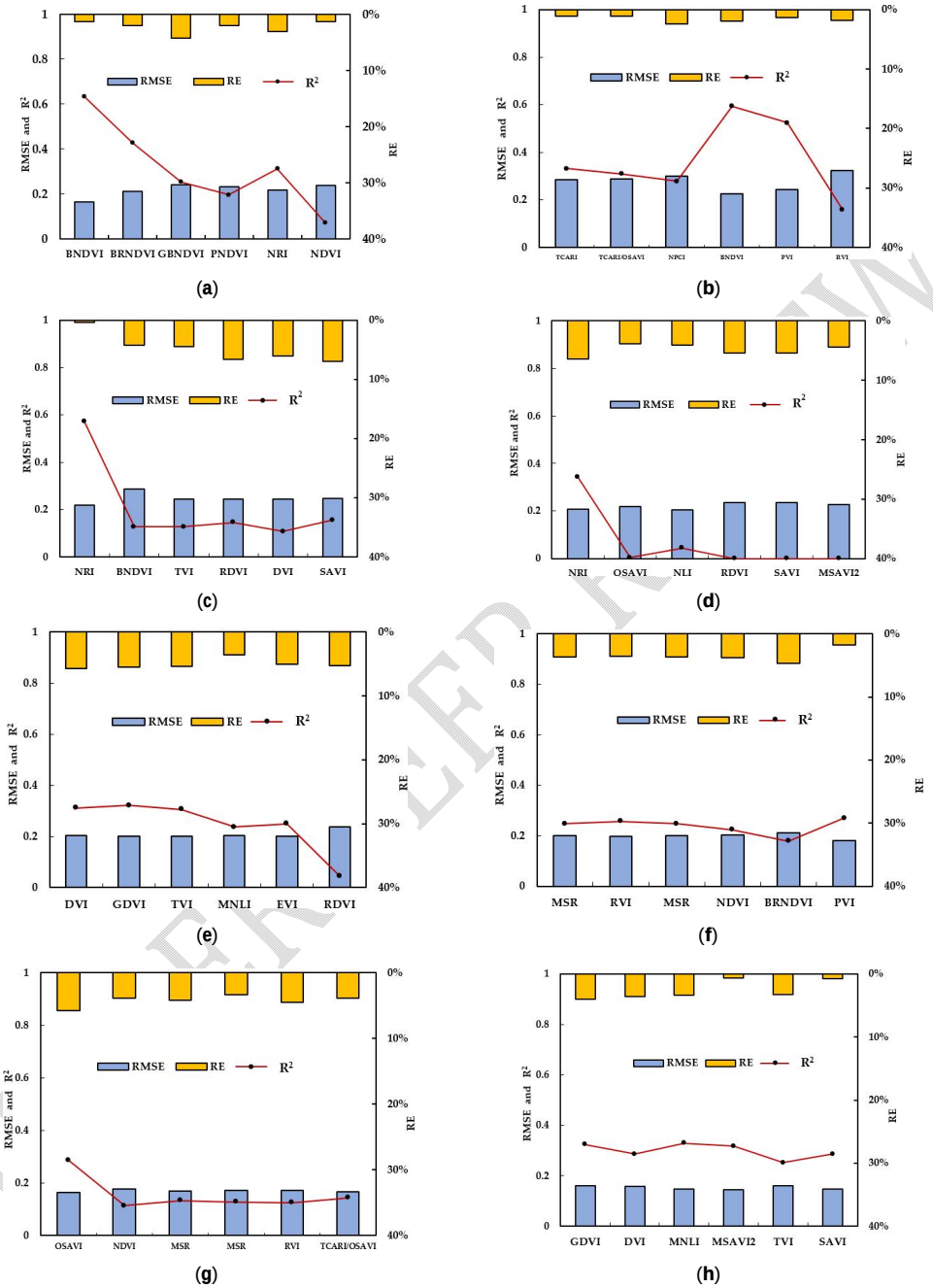

Figure3. Thetopsixmultispectralindicesofsummermaizeatthe V6(**a**),V10(**b**),V12(**c**),VT(**d**),R1(**e**),R2(**f**),R3(**g**),andR6(**h**)growthstagesandtheirlifecyclediagnosticevaluation.

To further verify the regional practicability of the multispectral plant nitrogen model at different stages, field verification was undertaken using the 2019 UAV multispectral data from V6 to R3 across seven stages. Table 4 shows the results. The RMSE values of the top six multispectral index diagnostic models at three stages (V6, V10, and R1) were between 0.01% and 0.31%. The errors were relatively small, with the RE values being within 10%. Therefore, the appropriate spectral index and its model could be determined based on the R^2 value in these three stages. The six spectral indices of PNDVI, NDVI, BRNDVI, GBNDVI, BNDVI, and NRI in stage V6 all maintained high accuracy (R^2>0.68); among these, the accuracy of GBNDVI was particularly high. The accuracy of TCARI in stage V10 was relatively good (R^2 = 0.547). In stage V12, NRI (R^2 = 0.612) was significantly better than that in the other indices (R^2<0.30). The prediction level of stage VT was very poor. TVI was better (R^2= 0.648) in stage R1. In the R2 and R3 stages, the RMSE values lay between 0.01% and 0.31%; however, the RE values were well over 30%. These results indicated that these models were unstable and had large errors.

Table 4. Results of UAV multispectral diagnosis and evaluation of nitrogen in summer maize at different growth stages.

Growth Stage	Multispectral Index	Relationship	RMSE(%)	RE(%)	R^2
V6	BNDVI	y = 0.443x+ 1.801	0.28	5.15	0.798
	BRNDVI	y = 0.551x+ 1.453	0.24	4.13	0.843
	GBNDVI	y = 0.734x+ 1.162	0.26	5.97	0.833
	PNDVI	y = 0.559x+ 1.434	0.23	3.88	0.861
	NRI	y = 0.491x+ 1.707	0.24	2.99	0.689
	NDVI	y = 0.324x+ 2.224	0.31	5.27	0.845
V10	TCARI	y = 0.590x+ 1.085	0.03	5.42	0.547
	TCARI/OSAVI	y = 0.223x+ 1.817	0.01	4.11	0.292
	NPCI	y=−0.169x+3.105	0.05	8.83	0.211
	BNDVI	y = 0.384x+ 1.709	0.06	7.59	0.277
	PVI	y = 0.176x+ 2.031	0.01	0.14	0.307
	RVI	y = 0.361x+ 1.643	0.04	2.67	0.249
V12	NRI	y=0.997x–0.244	0.31	9.51	0.612
	BNDVI	y = 0.265x+ 1.517	0.49	16.11	0.143
	TVI	y = 0.242x+ 1.700	0.37	11.42	0.232
	RDVI	y = 0.315x+ 1.469	0.40	12.86	0.282
	DVI	y = 0.230x+ 1.699	0.40	12.66	0.225
	SAVI	y = 0.334x+ 1.408	0.41	13.32	0.283
VT	NRI	y=−0.011x+0.216	1.53	88.51	0.001
	OSAVI	y=−0.025x+2.742	1.02	57.83	0.002
	NLI	y=−0.111x+2.762	0.92	50.34	0.010
	RDVI	y=−0.015x+2.299	0.61	32.92	0.002
	SAVI	y=−0.014x+2.575	0.87	49.14	0.001
	MSAVI2	y=−0.0045x+2.347	0.67	36.73	0.001

Formatted: Spanish (Mexico)

Table4. *Cont.*

GrowthStage	MultispectralIndex	Relationship	RMSE(%)	RE(%)	R^2
R1	DVI	y = 0.408x+ 0.757	0.18	7.24	0.636
	GDVI	y = 0.333x+ 0.846	0.20	8.52	0.602
	TVI	y = 0.447x+ 0.718	0.16	6.00	0.648
	MNLI	y = 0.259x+ 0.947	0.21	9.03	0.536
	EVI	y = 0.329x+ 0.890	0.18	5.98	0.611
	RDVI	y = 0.260x+ 0.911	0.23	11.49	0.578
R2	MSR	y = 0.608x+ 1.453	0.99	79.54	0.689
	RVI	y = 0.851x+ 1.569	1.40	113.3	0.698
	MSR	y = 0.695x+ 1.611	1.25	101.1	0.706
	NDVI	y = 0.383x+ 1.680	0.94	75.57	0.727
	BRNDVI	y = 0.253x+ 1.727	0.84	66.38	0.715
	PVI	y = 0.263x+ 1.695	0.82	64.84	0.707
R3	OSAVI	y = 0.081x+ 1.192	0.43	46.47	0.081
	NDVI	y = 0.185x+ 1.140	0.46	50.76	0.532
	MSR	y = 0.303x+ 0.947	0.37	40.26	0.532
	MSR	y = 0.327x+ 1.306	0.74	84.31	0.533
	RVI	y = 0.269x+ 1.129	0.52	57.91	0.534
	TCARI/OSAVI	y = 0.481x+ 1.067	0.63	71.88	0.497

Formatted: Spanish (Mexico)

Formatted: Spanish (Mexico)

Formatted: Spanish (Mexico)

Formatted: Spanish (Mexico)

Formatted: Spanish (Mexico)

Formatted: Spanish (Mexico)

Formatted: Spanish (Mexico)

Formatted: Spanish (Mexico)

Formatted: Spanish (Mexico)

Formatted: Spanish (Mexico)

Formatted: Spanish (Mexico)

Formatted: Spanish (Mexico)

Formatted: Spanish (Mexico)

3.2.2. EvaluationofOptimizedFour-StageModel

The four growth stages in the optimized four-stage model mean that the entire growthperiod of summer maize was divided into four stages: V6, V10, V12, and VT to R6. Thefirst three stages (V6, V10, and V12) were evaluated in the previous section. The evaluationof the fourth stage model (VT to R6) was undertaken based on the UAV multispectral data.The results are shown in Table 5 and Figure 3. The accuracy (R^2) of the top six multispectralindex(MSAVI2,GRNDVI,MSR,NDVI,NRI,andVARI)diagnosticmodelsintheVTtoR6stageranged from0.311to0.735.ThespectralindexwiththehighestR^2wasMSAVI2,followed by NDVI (R^2 = 0.497). The RMSE values ranged from 0.22% to 0.53%, and theREvaluesrangedfrom6.32%to22.0%.Themultispectralindiceswithan RE<10%wereMSAVI2 and GRNDVI. Therefore, in the VT to R6 stage, the model established by theMSAVI2multispectralindexhadhighaccuracyandgoodstability.

Table5. EvaluationresultsofnitrogeninsummermaizeintheVTtoR6stages.

MultispectralIndex	UAVDataEvaluation			
	Relationship	RMSE(%)	RE(%)	R^2
MSAVI2	y=0.848x+0.331	0.22	6.38	0.735
GRNDVI	y=0.306x+1.962	0.53	6.88	0.491
MSR	y=0.121x+1.517	0.42	18.30	0.373
NDVI	y=0.085x+1.521	0.39	15.03	0.497
NRI	y=0.736x+0.689	0.49	21.83	0.332
VARI	y=0.787x+0.621	0.50	22.20	0.311

Figure4showstheevaluationoftheoptimalspectralindexpredictionmodelforthenitrogendiagnosisofsummermaizeatdifferentgrowthstages.Thedottedlinerepresents

the 1:1 line. It was better to divide the whole life cycle of summer maize into four stages todiagnose the nitrogen nutrition status. Figure 3a represented the V6 stage, and the optimumspectral index was GBNDVI. Figure 3b represented the V10 stage, and the optimum spectralindexwasTCARI.Figure3crepresentedtheV12stage,andtheoptimumspectralindexwas NRI.Figure3drepresentedtheVTtoR6stage,andtheoptimumspectralindexwasMSAVI2.

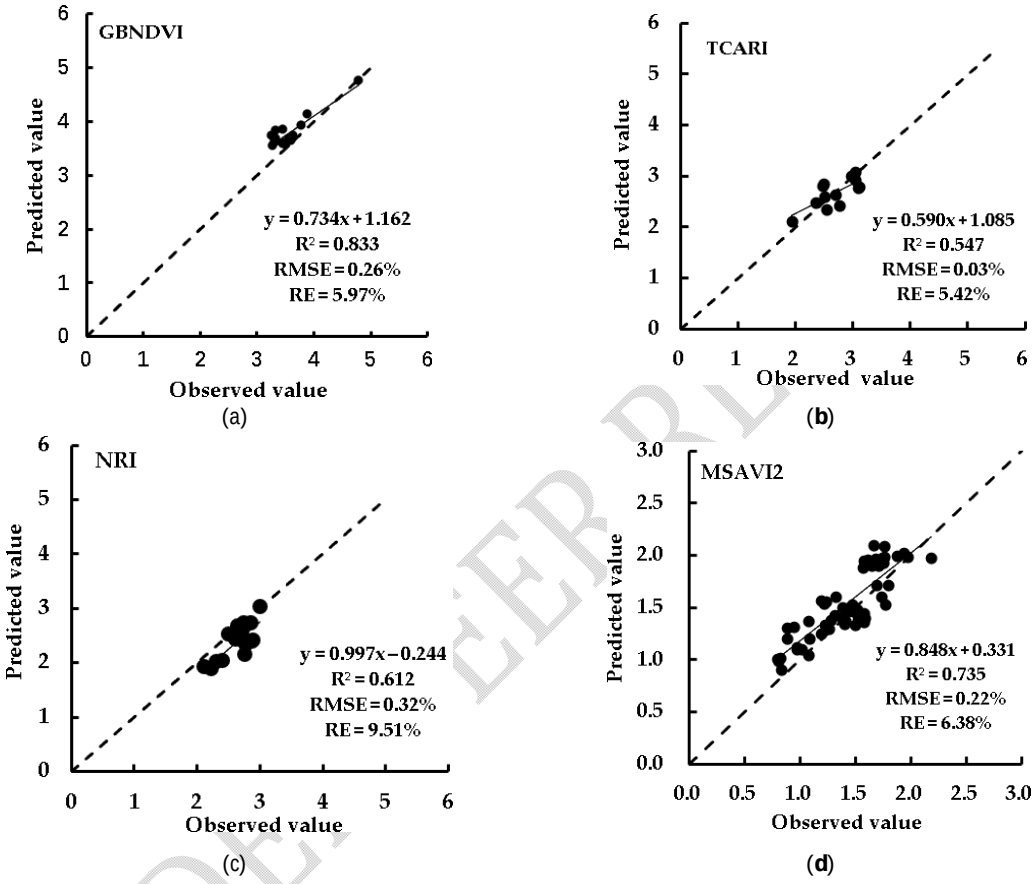

Figure 4. Evaluation results of the UAV multispectral nitrogen diagnosis models of summer maize attheV6(**a**),V10(**b**),V12(**c**),andVT-R6(**d**)growthstages.

In conclusion, the prediction accuracy of the nitrogen concentration in the whole lifecycle of summer maize using the four-stage model was higher, and it is in good agreementwith the actual observed value.Therefore, the four-stage model (Table 6) can be used tojointlypredictthenitrogenconcentrationinthelifecycleofsummermaize.

Comment [A1]: I suggest changing this word to summary or something similar.

Table6. A four-stage combined diagnostic model of nitrogen concentration in summer maize.

Growth Stage	Four-Stage Combined Diagnostic Model	
	Multispectral Index	Model
V6	GBNDVI	$y=-1.112\ln(x)+2.963$
V10	TCARI	$y=-0.0998x+2.228$
V12	NRI	$y=-5.833x+4.457$
VT-R6	MSAVI2	$y=2.116x^{0.879}$

Formatted: Spanish (Mexico)

Formatted: Spanish (Mexico)

3.3. Model Inversion Results Based on UAV Images

Combined with the UAV images, the monitoring and diagnosis of plant nitrogen concentration were undertaken based on the model established by the optimal multispectral index. Figure 4 shows the prediction results of each growth period. Moreover, the plant nitrogen concentrations estimated based on the appropriate multispectral index at different growth stages were consistent with the spatial distributions of the actual plant nitrogen concentration. The R^2 values of the regression equations established by the estimated and measured value at stages V6, V10, V12, and VT to R6 were 0.833, 0.547, 0.612, and 0.735, respectively. The TVI spectral index could be used to diagnose stage R1 in stage VT to R6 with an R^2 of 0.75. The prediction accuracies of stages V6, V12, and VT to R6 were higher than that of stage V10. Compared with the results of the satellite observation experiments, it was found that the prediction accuracy of this method was higher than that of the satellite observation experiments [47–49]. Furthermore, it could overcome the influence of satellite remote sensing by heavy field cycle [22] and weather cloud [18,27–30]. For example, Li, F.L. et al. [49] only estimated the leaf nitrogen content of winter wheat at the turning-green stage by ground hyperspectrum data combined with GF-1 satellite data, and the highest predictive determination coefficient was 0.59. The average determination coefficient of the model proposed in this study was 0.68.

According to the spectral diagnostic model and the critical nitrogen concentration of summer maize at different growth stages (Figure S3), the nitrogen nutrition status of field summer maize could be diagnosed based on the value range of the spectral index, as in Figure 5. At the V6 stage (Figure 5a), the corresponding value of the optimal spectral index (GBNDVI) corresponding to the critical nitrogen concentration was 0.61. At the V10 stage (Figure 5b), the corresponding value of the optimal spectral index (TCARI) was 2.73. At the V12 stage (Figure 5c), the corresponding value of the optimal spectral index (NRI) was 0.39. At the R1 stage (Figure 4d), the corresponding value of the optimal spectral index (TVI) was 21.63. At the R2 stage (Figure 5e), the corresponding value of the optimal spectral index (MSAVI2) was 0.55. At the R3 stage (Figure 5f) represented, the corresponding value of the optimal spectral index (MSAVI2) was 0.48. The nitrogen nutrition status of field summer maize could be diagnosed based on the value range of the spectral index.

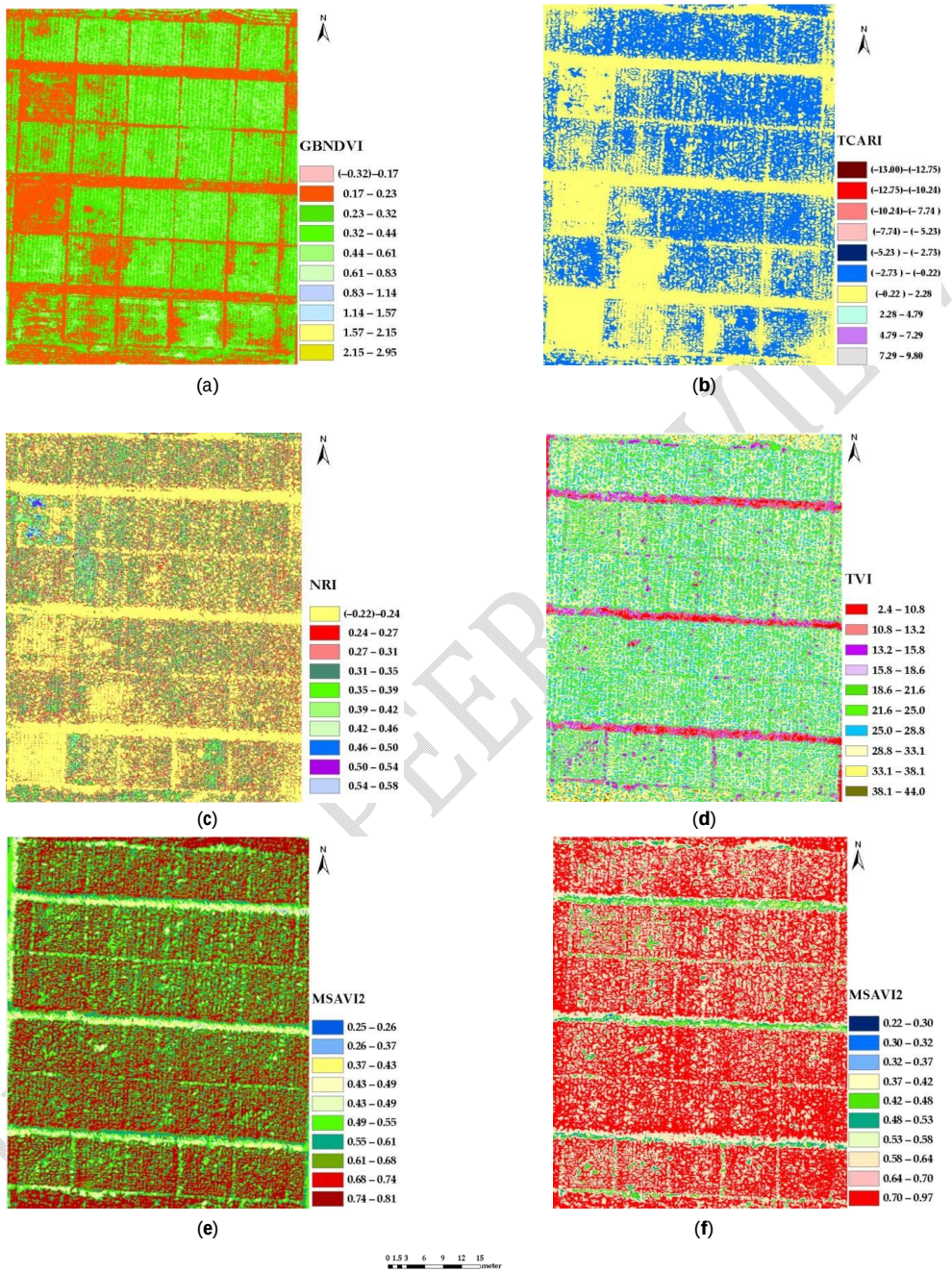

Figure 5. Spatial distribution of nitrogen diagnosis of summer maize plants by UAV at the V6 (**a**), V10 (**b**), V12 (**c**), R1 (**d**), R2 (**e**), and R3 (**f**) growth stages.

4. Discussion

4.1. Difficulties and Rationality of Experiment Implementation

This small-scale field trial, with well documented spatial differentiation of five different N-levels, enabled a case study for nitrogen concentration estimations based on acombination of near-ground hyperspectral data and UAV multispectral push scan scannerdata.Incomparisontootherstudiesusingsimilarspectraltechnology,thisstudycarriedout both near-ground hyperspectral trials that could facilitate accurate predictions andUAV multispectral trials with convenient and rapid prediction at a field scale; it was asuitable combination of both. The experiment lasted three years. As compared to othersimilarstudies[18,30,69–71],thechangesinnitrogenconcentration(FigureS3)andspectraldata during the life cycle of summer maize were observed here.The results provideddetailed experimental data for predicting nitrogen concentration by spectral technologyduringthelifecycleofsummermaizeandenabledamoreaccuratepredictionofnitrogenconcentrations.

4.2. Sensitivity, Validity, and Applicability of the Model

The proposed four-stage combined model (V6, V10, V12, and VT–R6) could be appliedmore effectively. The four-stage model was constructed based on the GBNDVI, TCARI, NRI,andMSAVI2spectralindices,whosefunctionswerelogarithmic,linear,linear,andpowerforeachspectralindex,respectively.Theformofmodelfunctionisconsistentwithotherresearch results [29,34,72,73]. To further analyze these indices, the sensitivity of the modelusing NE was discussed (Figure 6). The results indicated that the GBNDVI-based modeldemonstrated the lowest NE values, especially when the plant nitrogen concentrationsexceeded 4%. When the plant nitrogen concentration was <5%, the NE value was <0.5. TheTCARI-based model consistently demonstrated the second lowest NE for accessing plantnitrogen concentrations, especially those exceeding 1%.The NRI model demonstratedsimilarNEvaluestotheTCARIindex.Whentheplantnitrogenconcentrationswere<3%,the NE values of the TCARI and NRI models were <0.5. The MSAVI2 model had low NEvalues; however, as compared to the other three spectral indices, its NE value was thehighest.However, the NE was <0.1 when the plant nitrogen concentration was <2%.Due toa decrease in the plant nitrogen concentration with the advancement of the growth period(Figure S3), the GBNDVI, TCARI, NRI, and MSAVI2 models all showed high sensitivity intheirapplicationstage.

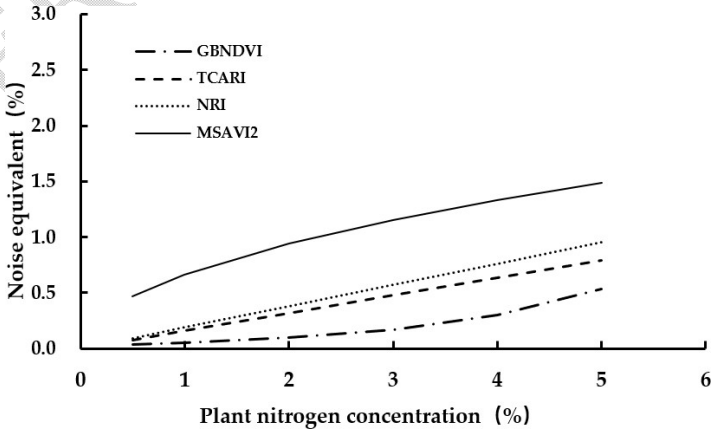

Figure6. Noiseequivalentofplantnitrogenconcentrationestimationbythespectralindices ofGBNDVI,TCARI,NRI,andMSAVI2.

In order to better highlight the validity of the four-stage model, we discussed thediagnosis of the nitrogen nutrition status of summer maize at different growth stages basedonthespectralindexcombinedwiththecriticalnitrogenconcentrationofsummermaize(Figure S3). At stage V6, the critical nitrogen concentration was 3.52%, and the correspond-ing GBNDVI value was 0.61; furthermore, the spectral index range corresponding to thenormalnitrogenconcentrationwas0.83–0.44(here,acriticalnitrogenconcentrationof 0.9to1.1timeswasconsideredasnormalnitrogenfertilizer;thatof>1.1timesasexcessnitrogen fertilizer; and that <0.9 times as deficient nitrogen fertilizer). At stage V10, thecritical nitrogen concentration was 2.50%, while the TCARI value was 0.22 to 5.23.At this stage, the summer maize grew rapidly, the demand for fertilizer increased, andthe differences between the different base fertilizer levels were significant. At stage V12,the critical nitrogen concentration was 2.2%, while the NRI was 0.42–0.35. The MSAVI2model was applied from the VT to R6 stage; however, the critical nitrogen concentrationwas significantly different in the VT, R1, R2, and R3–R6 stages (1.70%, 1.50%, 1.25%, and1%, respectively). Therefore, the corresponding MSAVI2 ranges were 0.69–0.87, 0.60–0.75,0.49–0.61,and0.42–0.53,respectively.ThespectralindexobtainedfromtheUAVsensordatahelpedtoeffectivelydiagnosethenitrogennutritionalstatusofsummermaize.

Theapplicabilityof thefour-stage modelwas furtherdiscussed consideringthe LAI.TheGBNDVImodelwassuitableforalowcoverofsummermaize.Atthisstage,theLAIwas<1;therewasmoreexposedsoil,andtheLAIvariedfrom0.34to0.94,withanaverageof0.67;moreover,thevegetationcoverwaslow.Sunetal.[74]foundthattheGBNDVIspectralindicescouldwellpredicttheabovegroundbiomassofrapeseed.Wangetal.[75]foundthattheGBNDVIindexmodelhelpedtobestpredictherbquantityintheYellowRiverwetlands.Theresultsofthesepreviousstudiesareconsistentwiththecurrentstudy.TheTCARImodelwassuitableinconsideringtherapidgrowthstageof summer maize. In this stage, the LAI varied from 1.11 to 2.51, with an average of 1.94;moreover, there was a low to medium cover of summer maize. Previous studies have foundthatchangesinthebackgroundreflectanceaffectthereflectanceslopebetween550and700 nm; furthermore, changes in the Rnir/Rg ratio in the TCARI calculation formula wereclosely related to the changes in the reflectance characteristics of the background material(soil and non-photosynthetic components). Cohen et al. [76] found that TCARI was stronglycorrelated with leaf N at the rapid growth stage. Therefore, TCARI is suitable for a low tomediumcoverageofsummermaize.TheNRImodelwassuitableforamediumtohighcover of summer maize. At this stage, the LAI of maize varied from 2.66 to 4.66, with anaverage of 3.61. The plants grew rapidly; however, their morphology was basically stable.The NRI is the normalized index of green and red light, which helps to better reflect thenitrogen nutrition status of crops at this stage.Wang et al. [77] found that the nitrogenconcentration in rice at the booting stage was also closely related to the NRI. The resultswere similar to those of this study.The MSAVI2 model was suitable for a high cover ofsummer maize. The LAI of maize changed from 3.13 to 4.74, with an average of 3.94; thechangewasinsignificantincomparisontothatofthepreviousstage.

4.3. FeasibilityofDataAcquisition

Only the growth stage of summer maize was determined when the four-stage modelwas applied in the field; moreover, the UAV sensor data were obtained.First, the corresponding diagnostic model was selected based on the stage; thereafter, the correspondingspectral index was calculated based on the spectral data. The nitrogen nutrition status ofsummer maize was diagnosed based on the range of normal fertilization. The model pro-posed here was simple, easy to calculate, and convenient for obtaining data. The UAV wasequippedwithamultispectralsensor.Comparedwiththehyperspectralsensor,althoughthehyperspectral sensor can obtain hundreds of narrow spectral bands at the same timewith high accuracy [35], the multispectral sensor can obtain spectral information on blue,green, red, near infrared, and red edge bands, including nitrogen-sensitive bands.Basically,itcanmeetourworkonthediagnosisofthenitrogennutritionstatusofcrops[17,34].

Furthermore, the cost was lower than that of a UAV equipped with a hyperspectral sensor [15,44].It was convenient for a wide range of people and a wide range of regionalapplications[30,32,37].

4.4. LimitationsoftheMethodandtheFocusofFutureWork

Inordertoanalyzetheinterannualapplicabilityofthemodel,thisstudyonlycarriedouta3-yearstudybasedonthesamevarietyofsummermaize. Thismethodhasacertainreferencevalueforothervarietiesandothercropsinthecarryingoutofsimilarresearch.However, it should be noted that, firstly, as different crop types, there will be differencesin the division of the growth stages; secondly, different crop types may have differentsensitive bands and appropriate spectral indices. Further tests involving different varietiesofmaizeandawiderangeofvegetationtypesandregionalscalesshouldbeconsidered toverify the use of spectral indices in determining the nitrogen content in plants. To facilitatethe application of the model, this study only analyzed the unitary model; moreover, furtherstudies on the multivariate model could be undertaken. Consideration of a combinationoftheradiativetransfermodelandthestatisticalmodelisalsopromisingingoing ahead.This study undertook three years of experiments, which could be further carried out in thefuturetosupplementthesamples,furtherimprovethemodel,andexpanditsapplications.

5. Conclusions

In this research work~~Here~~, ground hyperspectral technology was combined with UAV multispectral tech-nology; thereafter, a multi-index synergy model of nitrogen concentration during the lifecycle of summer maize was proposed based on the data of a 3-year systematic field experi-ment. Based on the critical nitrogen concentration model, the spectral index thresholds ofsufficientnitrogenlevelsweredeterminedatdifferentstages.

The results of this study showed that the optimized four-stage, multi-index synergymodel could better diagnose the nitrogen nutrition status considering the entire life cycle ofsummer maize. GBNDVI was suitable for stage V6 with low coverage (mean LAI = 0.67),the evaluation accuracy $R^2$was 0.833, while the spectral index threshold of nitrogenadequacy ranged from 0.83 to 0.44. TCARI was suitable for stage V10 with medium andlow coverage (mean LAI = 1.94), with an $R^2$of 0.547.The spectral index threshold ofnitrogen adequacy ra~~n~~nged fro~~m~~0.22 to5.23.NRI was suitable for stage V12 withmedium to high coverage (mean LAI = 3.61), and with an R^2 of 0.612. The spectral indexthreshold of nitrogen adequacy was 0.42–0.35. MSAVI2 was suitable for stage VT–R6 withhigh coverage (mean LAI = 3.94), and with an R^2 of 0.735. The spectral index thresholds ofnitrogenadequacyinstagesVT,R1,R2,andR3-R6were0.69–0.87,0.60–0.75,0.49–0.61,and0.42–0.53,respectively.

The nitrogen concentration of summer maize plants simulated by the optimal multispectral index synergy model constructed at the different growth stages was similar totheactualspatialdistribution.Thisstudyprovidestechnicalsupportforthetimely,rapid,convenient, and accurate diagnosis of summer maize nitrogen nutrition and provides abasisfortheSCMofnitrogen.

Supplementary Materials: The following supporting information can be downloaded at:https://www.mdpi.com/article/10.3390/atmos13010122/s1, Table S1: number of experimental observations(n), tissue sampling date, hyperspectral acquisition date and local time, UAV sampling area and localtime, Table S2: nitrogen concentration of summer maize plants, Figure S1: UAV aerial photographyoperations, Figure S2: UAV route, Figure S3: relationship between plant critical nitrogen concentrationand crop biomass of summer maize. "•" represented the data in 2017. "×" represented the data in2018."▲"representedthedatain2019.

InstitutionalReviewBoardStatement: Notapplicable.

InformedConsentStatement: Notapplicable.

DataAvailabilityStatement: Notapplicable.

References

1. Duarte, A.G.; Longstaffe, F.J.; Way, D.A. Nitrogen fertilisation influences low CO_2 effects on plant performance. *Funct. Plant Biol.* **2020**, *47*, 134–144. [CrossRef]
2. Dier, M.; Hüther, L.; Schulze, W.X.; Erbs, M.; Koehler, P.; Weigel, H.-J.; Manderscheid, R.; Zörb, C. Elevated atmospheric CO_2 concentration has limited effect on wheat grain quality regardless of nitrogen supply. *J. Agric. Food Chem.* **2020**, *68*, 3711–3721. [CrossRef]
3. Córcoles, H.L.; Juan, J.; Picornell, M.R. Biomass production and yield in irrigated maize at different rates of nitrogen in a semi-aridclimate. *NJAS-WangJ.LifeSci.* **2020**, *92*, 10032. [CrossRef]
4. Dong, K.W.; Riley, W.J.; Wu, Y. More fertilizer and impoverished roots required for improving wheat yields and profits underclimatechange. *FieldCropsRes.* **2020**, *249*, 107756.
5. Gao, Y.; Liang, A.; Zhang, Y.; Mclaughlin, N.; Fan, R. Dynamics of microbial biomass, nitrogen mineralization and crop uptake inresponse to placement of maize residue returned to chinese mollisols over the maize growing season. *Atmosphere* **2021**, *12*, 1166. [CrossRef]
6. Noh, H.; Zhang, Q.; Shin, B.; Han, S.; Feng, L. A neural network model of maize crop nitrogen stress assessment for a multi-spectralimagingsensor. *Biosyst. Eng.* **2006**, *94*, 477–485. [CrossRef]
7. Hatfield, J.L.; Gitelson, A.A.; Schepers, J.S.; Walthall, C.L. Applicationofspectralremotesensingforagronomicdecisions. *Agron. J.* **2008**, *100*, 117–131. [CrossRef]
8. Lu, D.J.; Lu, F.F.; Pan, J.X.; Cui, Z.N.; Zou, C.Q.; Chen, X.P.; He, M.; Wang, Z. Theeffectsofcultivarandnitrogenmanagementonwheatyieldand nitrogenuseefficiencyintheNorthChinaPlain. *FieldCropsRes.* **2015**, *171*, 157–164. [CrossRef]
9. Meng, Q.F.; Peng, H.; Wu, L.; Chen, X.P.; Cui, Z.L.; Zhang, F.S. UnderstandingproductionpotentialsandyieldgapsinintensivemaizeproductioninChina. *FieldCropsRes.* **2013**, *143*, 91–97. [CrossRef]
10. Wang, H.; Guo, Z.; Shi, Y.; Wang, H.G.; Zhen, W. Impactoftillagepracticesonnitrogenaccumulationandtranslocationinwheatandsoilnitrate-nitrogenleachingindrylands. *Soil Till. Res.* **2015**, *153*, 20–27. [CrossRef]
11. Serrano, L.; Filella, I.; Penuelas, J. Remotesensingofbiomassandyieldofwinterwheatunderdifferentnitrogensupplies. *Crop. Sci.* **2000**, *40*, 723–731. [CrossRef]
12. Luo, J.; Ma, R.; Feng, H.; Li, X. Estimatingthetotalnitrogenconcentrationofreedcanopywithhyperspectralmeasurementsconsidering a non-uniform vertical nitrogen distribution. *RemoteSens.* **2016**, *8*, 789. [CrossRef]
13. Huang, W.; Yang, Q.; Pu, R.; Yang, S. Estimation ofnitrogen verticaldistribution bybi-directional canopyreflectance inwinterwheat. *Sensors* **2004**, *14*, 20347–20359. [CrossRef] [PubMed]
14. Kayad, A.; Sozzi, M.; Gatto, S.; Whelan, B.; Sartori, L.; Marinello, F. Tenyearsofcornyielddynamicsatfieldscaleunderdigitalagricultures olutions: Acasestudyfromnorth Italy. *Comput. Electron. Agric.* **2021**, *185*, 106126. [CrossRef]
15. Wei, P.F.; Xu, X.G.; Li, Z.Y.; Yang, G.J.; Li, Z.H.; Feng, H.K.; Chen, G.; Fan, L.L.; Wang, Y.L.; Liu, S.B. Remote sensing estimation ofnitrogen content in summer maize leaves based on multispectral images of UAV. *Trans. Chin. Soc. Agric. Eng.* **2019**, *35*, 126–133. (InChinese)
16. Jeong, H.; Bhattarai, R. Exploringtheeffectsofnitrogenfertilizationmanagementalternativesonnitratelossandcropyieldsintile-drained fields in Illinois. *J. Environ. Manag.* **2018**, *213*, 341–352. [CrossRef] [PubMed]
17. Colorado, J.D.; Cera-Bornacelli, N.; Caldas, J.S.; Petro, E.; Jaramillo-Botero, A. Estimation of nitrogen in rice crops from UAV-capturedimages. *RemoteSens.* **2020**, *12*, 3396. [CrossRef]
18. Corti, M.; Cavalli, D.; Cabassi, G.; Vigoni, A.; Degano, L.; Gallina, P.M. Application of a low-cost camera on a UAV to estimatemaizenitrogen-related variables. *Precis. Agric.* **2019**, *20*, 675–696. [CrossRef]
19. Olfs, H.-W.; Blankenau, K.; Brentrup, F.; Jasper, J.; Link, A.; Lammel, J. Soil-andplant-basednitrogen-fertilizerrecommendationsinarablefarming. *J. PlantNutr. Soil. Sci.* **2005**, *168*, 414–431. [CrossRef]
20. Li, L.T.; Wang, S.Q.; Ren, T.; Wei, Q.Q.; Ming, J.; Li, J.; Li, X.; Cong, R.; Lu, J. Ability of models with effective wavelengths tomonitornitrogenandphosphorusstatusofwinteroilseedrapeleavesusinginsitucanopyspectroscopy. *FieldCropsRes.* **2018**, *215*, 173–186. [CrossRef]

21. Chen,P.F.;Haboudane,D.;Tremblay,N.;Wang,J.H.;Vigneault,P.;Li,B.G.Newspectralindicatorassessingtheefficiencyofcropnitrogentreatmentincornandwheat.*RemoteSens.Environ.***2010**,*114*,1987–1997.[CrossRef]
22. Wójtowicz,M.;Wójtowicz,A.;Piekarczyk,J.Applicationofremotesensingmethodsinagriculture.*Commun.Biol.CropSci.***2016**, *11*,31–50.
23. Li,F.;Miao,Y.;Hennig,S.D.;Gnyp,M.L.;Chen,X.P.;Jia,L.L.;Bareth,G.Evaluatinghyperspectralvegetationindicesforestimatingnitrogenconcentrationofwinterwheatatdifferentgrowthstages.*Precis.Agric.***2010**,*11*,335–357.[CrossRef]
24. Lulu,M.;Xin,L.;Ze,Z.Establishmentofnitrogennutritiondiagnosismodelfordrip-irrigationcottonbasedoncriticalnitrogenconcentration.*Trans.Chin.Soc.Agric.Eng.***2018**, *49*, 277–284.(In Chinese)
25. Mistele,B.;Schmidhalter,U.Estimatingthenitrogennutritionindexusingspectralcanopyreflectancemeasurements.*Eur.J.Agron.***2008**,*29*,184–190.[CrossRef]
26. Bagheri,N.;Ahmadi,H.;Alavipanah,S.K.;Omid,M.Multispectralremotesensingforsite-specificnitrogenfertilizermanagement. *Pesqui.Agropecu.Bras.***2013**,*48*,1394–1401.[CrossRef]
27. Sims,D.A.;Gamon,J.A.Relationshipsbetweenleafpigmentcontentandspectralreflectanceacrossawiderangeofspecies,leafstructuresanddevelopmental stages.*RemoteSens.Environ.***2002**,*81*, 337–354.[CrossRef]
28. Zhang,J.J.;Du,P.;Guo,J.B.;Cao,R.;Zhang,J.;Ma,X.M.StudyofcriticalnitrogenconcentrationmodelandnitrogennutritiondiagenosisinwinterwheatwithdifferentNefficiency.*J.TriticeaeCrops***2017**,*11*,86–94.(InChinese)
29. Palka, M.; Manschadi, A.M.;Koppensteiner, L.; Neubauer, T.;Fitzgerald, G.J. Evaluatingthe performance of theCCCI-CNI indexfor estimating Nstatus of winterwheat.*Eur.J.Agron.***2021**, *130*,126346.[CrossRef]
30. Nigon,T.J.;Yang,C.;Paiao,G.D.;Mulla,D.J.;Fernández,F.G.Predictionofearlyseasonnitrogenuptakeinmaizeusinghigh-resolutionaerialhyperspectralimagery.*RemoteSens.***2020**,*12*,1234.[CrossRef]
31. Geipel,J.;Link,J.;Wirwahn,J.A.;Claupein,W.Aprogrammableaerialmultispectralcamerasystemforin-seasoncropbiomassandnitrogencontentestimation.*Agriculture***2016**,*6*,4.[CrossRef]
32. Huang, Y.; Thomson, S.J.; Lan, Y.; Maas, S.J. Multispectral imaging systems forairborne remote sensing to support agriculturalproductionmanagement.*Int.J.Agric.Biol.Eng.***2010**,*3*,50–62.
33. Ge,H.;Xiang,H.;Ma,F.;Li,Z.;Du,C.EstimatingplantnitrogenconcentrationofricethroughfusingvegetationindicesandcolormomentsderivedfromUAV-RGBimages.*RemoteSens.***2021**,*13*,1620.[CrossRef]
34. Wang,Y.P.;Chang,Y.C.;Shen,Y.Estimationofnitrogenstatusofpaddyriceatvegetativephaseusingunmannedaerialvehiclebasedmultispectralimagery.*Precis.Agric.***2021**,*23*,1–17.[CrossRef]
35. Tao,H.;Feng,H.;Xu,L.;Miao,M.;Yang,G.;Yang,X.Estimationoftheyieldandplantheightofwinterwheatusing UAV-basedhyperspectralimages.*Sensors***2020**,*20*,1231.[CrossRef]
36. Gilliot, J.M.; Michelin, J.; Hadjard, D.; Houot, S. An accurate method for predicting spatial variability of maize yield fromUAV-based plant height estimation:A tool for monitoring agronomic field experiments.*Precis.Agric.***2021**, *22*, 897–921.[CrossRef]
37. Caturegli,L.;Corniglia,M.;Gaetani,M.;Grossi,N.;Magni,S.;Migliazzi,M.;Angelini,L.;Mazzoncini,M.;Silvestri,N.;Fontanelli, M.Unmannedaerialvehicletoestimatethenitrogenstatusofturfgrasses.*PLoSONE***2016**,*11*,e0158268.
38. Liu,H.Y.;Zhu,H.;Wang,P.Quantitativemodelingforleafnitrogencontentofwinterwheatusing UAV-basedhyperspectraldata. *Int.J.RemoteSens.***2017**, *38*,2117–2134.[CrossRef]
39. Hunt, E.R.; Horneck, D.A.; Spinelli, C.B.; Turner, R.W.; Bruce, A.E.; Gadler, D.J. Monitoring nitrogen status of potatoes usingsmall unmannedaerialvehicles.*Precis.Agric.***2018**,*19*,314–333.[CrossRef]
40. Singh,S.K.;Houx,J.H.;Maw, M.J.W.;Fritschi,F.B.Assessmentofgrowth,leafNconcentrationandchlorophyllcontentofsweetsorghum usingcanopyreflectance.*FieldCropsRes.***2017**,*209*, 47–57.[CrossRef]
41. Sylvain, J.; Fabienne, M.; Ryad, B.; Nathalie, G. Retrieving LAI, chlorophyll and nitrogen contents in sugar beet crops frommultiangular optical remote sensing: Comparison of veg- etation indices and PROSAIL inversion for field phenotyping. *FieldCropsRes.***2017**,*210*,33–46.
42. Liu, C.H.; Ma, W.Y.; Chen, Z.C.; Wang, C.Y.; Lu, J.J.; Yue, X.Z.; Wang, Z.; Fang, Z.; Miao, Y. Nitrogen nutrition diagnosis of winterwheat based on the UAV remote sensing.*J.HenanPoly.Univ.***2018**, *37*, 45–53.(In Chinese)
43. Swain, K.C.; Thomson, S.J.; Jayasuriya, H.P. Adoption of an unmanned helicopter for low-altitude remote sensing to estimateyield andtotalbiomass ofaricecrop.*Trans.ASABE***2010**,*53*,21–27.[CrossRef]
44. Gabriel,J.L.;Zarco-Tejada,P.J.;López-Herrera,P.J.;Perez-Martín,E.;Alonso-Ayuso,M.;Quemada,M.Airborneandgroundlevelsensorsformonitoringnitrogenstatusinamaizecrop.*Biosyst.Eng.***2017**,*160*,124–133.[CrossRef]
45. Diker,K.;Bausch,W.C.PotentialUseofNitrogenReflectanceIndextoestimatePlantParametersandYieldofMaize.*Biosyst.Eng.* **2003**,*85*, 437–447.[CrossRef]
46. He,D.; Wang, E.; Wang, J.; Robertson, M.J. Datarequirementfor effective calibration of process-basedcropmodels.*Agric.For.Metorol.***2017**,*234*,136–148.[CrossRef]
47. Mittermayer,M.;Gilg,A.;Maidl,F.X.;Ntscher,L.;Hülsbergen,K.J.Site-specificnitrogenbalancesbasedonspatiallyvariablesoiland plantproperties.*Precis.Agric.***2021**,*22*,1416–1436.[CrossRef]
48. Huang,S.;Miao,Y.;Yuan,F.;Martin,G.;Yao,Y.;Qiang,C.Potentialofrapideyeandworldview-2satellitedataforimprovingricenitrogenstatusmonitoringatdifferentgrowthstages.*RemoteSens.***2017**,*9*,227.[CrossRef]

49. Li,F.L.;Chang,Q.R.;Shen,J.;Wang,L.Remotesensingestimationofwinterwheatleafnitrogencontentbasedon GF-1satellitedata.*Trans.Chin.Soc.Agric.Eng.***2016**,*32*,157–164.(InChinese)
50. Cao,Q.;Miao,Y.M.;Li,F.;Gao,X.W.;Liu,B.;Lu,D.J.;Chen,X.P. Developing a new crop circle active canopy sensor-basedprecisionnitrogenmanagementstrategyforwinterwheatintheNorthChinaPlain.*Precis.Agric.***2016**,*18*,2–18.[CrossRef]
51. Chen,J.M.Evaluationofvegetationindicesandmodifiedsimpleratioforborealapplications.*Can.J.RemoteSens.***1996**,*22*, 229–242.[CrossRef]
52. Daughtry,C.S.T.;Walthall,C.L.;Kim,M.S.Estimatingcornleafchlorophyllconcentrationfromleafandcanopyreflectance. *RemoteSens.Environ.***2000**,*74*,229–239.[CrossRef]
53. Tucker, C.J. Red and photographic infrared linear combinations for monitoring vegetation. *Remote Sens. Environ.* **1979**, *8*, 127–150.[CrossRef]
54. Gitelson, A.A.; Kaufman, Y.J.; Stark, R.; Rundquista, D. Novel algorithms for remote estimation of vegetation fraction. *RemoteSens.Environ.***2002**,*80*,76–87.[CrossRef]
55. Gong, P.; Pu, R.; Biging, G.S.; Larrieu, M.R. Estimation of forest leaf area index using vegetation indices derived from Hyperionhyperspectraldata.*IEEETrans.Geosci.RemoteSens.***2003**,*41*,1355–1362.[CrossRef]
56. Haboudane, D.; Miller, J.R.; Tremblay, N.; Zarco-Tejada, P.J.; Dextraze, L. Integrated narrow—Band vegetation indices forpredictionofcropchlorophyllcontentforapplicationtoprecisionagriculture.*RemoteSens.Environ.***2002**,*81*,416–426.[CrossRef]
57. Haboudane, D.; Miller, J.R.; Pattey, E.; Zarco-Tejada, P.J.; Strachan, I.B. Hyperspectral vegetation indices and novel algorithms forpredicting green LAI of crop canopies: Modeling and validation in the context of precision agriculture. *Remote Sens. Environ.***2004**,*90*,337–352.[CrossRef]
58. Huete,A.R.Asoiladjustedvegetationindex SAVI.*RemoteSens.Environ.***1988**,*25*,295–309.[CrossRef]
59. Jordan,C.F.Derivationofleaf—Areaindexfromqualityoflightontheforestfloor.*Ecology***1969**,*50*,663–666.[CrossRef]
60. Liu, H.Q.; Huete, A.A. Feedback-based modification of the NDVI to minimize canopy background and atmospheric noise.*IEEETrans.Geosci.RemoteSens.***1995**,*33*,457–465.[CrossRef]
61. Navarro, G.; Caballero, M.; Silva, G.; Parra, P.C.; Águeda, V.; Caldeira, R.M.A. Evaluation of forest fire on Madeira Island usingSentinel-2A MSIimagery.*Int.J.Appl.Earth.OBS***2017**,*58*, 97–106.[CrossRef]
62. Penuelas, J.; Gamon, J.A.; Fredeen, A.L.; Merino, J.; Field, C.B. Reflectance indices associated with physiological changes innitrogenandwater-limitedsunflowerleaves.*RemoteSens.Environ.***1994**,*48*,135–146.[CrossRef]
63. Qi,J.;Chehbouni,A.;Huete,A.R.;Kerr,Y.H.;Sorooshian,S.Amodifiedsoiladjustedvegetationindex(MSAVI).*RemoteSens.Environ* .**1994**,*48*,119–126.[CrossRef]
64. Rouse, J.W.; Haas, R.H.; Schell, J.A.; Deering, D.W.; Harlan, J.C. Monitoring the vernal advancements and retrogradation ofnatural vegetation.*NASA/GSFCT Type III Final.Rep.***1974**, 1.Available online:https://ntrs.nasa.gov/citations/19730017588(accessedon27November2021).
65. Schleicher,T.D.;Bausch,W.C.;Delgado,J.A.;Ayer,P.D.Evaluationandrefinementofthenitrogenreflectanceindex(NRI)forsitespecific fertilizermanagement.InProceedingsofthe2001ASAEAnnualInternationalMeeting,Sacramento,CA,USA,30July–1August2001.
66. Li, X.C.; Xu, X.G.; Bao, Y.S.; Huang, W.J.; Luo, J.H.; Dong, Y.Y.; Song, X.Y.; Wang, J.H. Retrieving LAI of Winter Wheat Based onSensitiveVegetationIndexbytheSegmentationMethod.*Sci.Agric.***2012**,*45*,3486–3496.(InChinese)
67. Wang,F.M.;Huang,J.F.;Tang,Y.I.;Wang,X.Z.Newvegetationindexanditsapplicationinestimatingleafareaindexofrice.*Chin. J.RiceSci.***2007**,*21*,159–166.(InChinese)[CrossRef]
68. Viña,A.;Gitelson,A.A.;Nguy-Robertson,A.L.;Peng,Y.Comparisonofdifferentvegetationindicesfortheremoteassessmentofgreenleaf areaindex ofcrops.*RemoteSens.Environ.***2011**,*115*, 3468–3478.[CrossRef]
69. Fan,L.;Zhao,J.;Xu,X.;Liang,D.;Yang,G.;Feng,H.;Yang,H.;Wang,Y.;Chen,G.;Wei,P.Hyperspectral-BasedEstimationofLeafNitrogenContentinCornUsingOptimalSelectionofMultipleSpectralVariables.*Sensors***2019**,*19*,2898.[CrosRef]
70. Torino,M.S.;Ortiz,B.V.;Fulton,J.P.;Balkcom,K.S.;Wood,C.W.Evaluationofvegetationindicesforearlyassessmentofcornstatusandyieldpotentialinthesoutheasternunitedstates.*Agron.J.* **2014**,*106*,1389–1401.[CrossRef]
71. Li,F.;Miao,Y.;Feng,G.;Yuan,F.;Yue,S.;Gao,X.;Liu,Y.;Liu,B.;Ustin,S.L.;Chen,X.Improvingestimationofsummermaizenitrogenstatus withrededge-basedspectralvegetationindices.*FieldCropsRes.* **2014**,*157*,111–123.[CrossRef]
72. Osco,L.P.;José,M.J.;Ramos,A.P.M.;Furuya,D.E.G.;Teodoro,P.E.Leafnitrogenconcentrationandplantheightpredictionformaizeusin gUAV-basedmultispectralimageryandmachinelearningtechniques.*RemoteSens.***2020**,*12*,3237.[CrossRef]
73. Lu,J.;Cheng,D.;Geng,C.;Zhang,Z.;Xiang,Y.;Hu,T.Combiningplantheight,canopycoverageandvegetationindexfromuav-basedrgbimagestoestimateleafnitrogenconcentrationofsummermaize. *Biosyst.Eng.***2021**,*202*,42–54. [CrossRef]
74. Sun,J.Y.;Huang,Y.;Cao,H.X.;Jiao,Y.G.Correlationanalysisbetweenabovegroundbiomassofrapeandcanopyspectralvegetationinde x.*Guangxi Agric.Sci.***2009**,*40*,716–723.(InChinese)
75. Wang,J.B.;Zhang,J.;Ma,Y.Studyontheabovegroundvegetationbiomassestimationmodelbasedon GF-1WFVsatelliteimageintheYellowRiverestuarywetland.*ActaLaser Biol.Sin.***2014**,*23*,604–608.(InChinese)

76. Cohen, Y.; Alchanatis, V.; Zusman, Y.; Dar, Z.; Onfil, D.J.; Karnieli, A.; Zilberman, A.; Moulin, A.; Ostrovsky, V.; Levi, A.; et al.Leafnitrogenestimationinpotatobasedonspectraldataandonsimulatedbandsoftheμsatellite. *Precis.Agric.***2010**,*11*,520–537.[CrossRef]
77. Wang, W.; Yao, X.; Yao, X.; Tian, Y.; Liu, X.; Ni, J.; Cao, W.; Zhu, Y. Estimating leaf nitrogen concentration with three-bandvegetation indicesinriceand wheat.*FieldCropsRes.***2012**, *129*,90–98.[CrossRef]